

## Past permafrost dynamics can inform future permafrost carbon-climate feedbacks

Miriam C. Jones <sup>1</sup>✉, Guido Grosse <sup>2</sup>, Claire Treat <sup>2</sup>, Merritt Turetsky <sup>3</sup>,  
Katey Walter Anthony <sup>4</sup> & Laura Brosius <sup>4</sup>

Climate warming threatens to destabilize vast northern permafrost areas, potentially releasing large quantities of organic carbon that could further disrupt the climate. Here we synthesize paleorecords of past permafrost-carbon dynamics to contextualize future permafrost stability and carbon feedbacks. We identify key landscape differences between the last deglaciation and today that influence the response of permafrost to atmospheric warming, as well as landscape-level differences that limit subsequent carbon uptake. We show that the current magnitude of thaw has not yet exceeded that of previous deglaciations, but that permafrost carbon release has the potential to exert a strong feedback on future Arctic climate as temperatures exceed those of the Pleistocene. Better constraints on the extent of subsea permafrost and its carbon pool, and on carbon dynamics from a range of permafrost thaw processes, including blowout craters and megaslumps, are needed to help quantify the future permafrost-carbon-climate feedbacks.

In recent years, permafrost thaw has captivated the attention of scientists and the public, alike, highlighting the potential impacts of the release of carbon and pathogens like anthrax. A major concern is the potential role that permafrost thaw will play in causing feedbacks to climate change, given the sheer size of the permafrost region soil carbon pool (1330–1580 Pg C, excluding subsea permafrost)<sup>1,2</sup>, which is 55–68% greater than the 2020 atmospheric C pool (>860 Pg C)<sup>3</sup>. The large uncertainty of how much carbon might be mobilized by thaw in a warming climate has led to dramatic descriptions of permafrost carbon vulnerability as “A sleeping giant”<sup>4</sup>, “Pandora’s freezer”<sup>5</sup>, or a potential “Carbon bomb”<sup>6,7</sup> that could rapidly destabilize the climate system. Because of this potential, some studies introduced permafrost as a probable tipping element in the Earth System<sup>8–10</sup>. Contrastingly, some view permafrost as a rather stable or only slowly reacting component in the climate system on millennial timescales, suggesting that even with release of substantial carbon, the slow timescale of release would be compensated by other components of the Earth system (vegetation, peat, ocean), resulting in minimal feedback to climate. This has led to the conclusion that permafrost carbon could therefore not be an important factor in abrupt carbon cycle shifts when compared to human-driven, oceanic, or terrestrial tropical components<sup>11–13</sup>. With atmospheric CO<sub>2</sub> concentrations now reaching nearly 420 ppm, values not observed in the last 3 million years, and expected to reach concentrations not observed in 30 million years by 2300 under high emissions scenarios<sup>14</sup>, there is now even more urgency to understand the consequences and associated feedbacks to climate<sup>15</sup> from the warming and thaw of this large permafrost carbon pool<sup>2,15</sup>. Furthermore, permafrost carbon dynamics are not yet included in most IPCC Earth system models<sup>16</sup>, and this omission suggests that even with the strictest emission reductions, climate targets could be overshoot<sup>17,18</sup>. Recent field, remote sensing, and modeling studies point at increasingly rapid

<sup>1</sup>Florence Bascom Geoscience Center, U.S. Geological Survey, Reston, VA 20192, USA. <sup>2</sup>Alfred Wegener Institute Helmholtz Center for Polar and Marine Research, Potsdam, Germany. <sup>3</sup>Institute of Arctic and Alpine Research, Ecology and Evolutionary Biology Department, University of Colorado Boulder, Boulder, CO, USA. <sup>4</sup>Water and Environmental Research Center, University of Alaska Fairbanks, Fairbanks, AK, USA. ✉email: [miriamjones@usgs.gov](mailto:miriamjones@usgs.gov)

degradation of permafrost on decadal scales<sup>19–27</sup>, but understanding how this recent permafrost destabilization compares to past periods of rapid climate change, such as during the last deglaciation, and the impacts to global climate, remain limited.

While glacial cooling happened gradually over millennia, deglaciation was punctuated by rapid, or even abrupt, warming, when a series of positive feedbacks in response to gradual changes in solar insolation, tipped earth system components into a new state, often causing substantial climate shifts in a matter of decades<sup>28</sup>. Here we evaluate whether permafrost dynamics associated with previous abrupt warming events can serve as potential analogs to future permafrost stability and impacts on carbon cycling in a rapidly warming climate. As each glaciation and associated climate shifts have in turn, bulldozed, buried, and eroded away much evidence of our climate history on land, we focus on terrestrial permafrost processes that influence climate since our most recent glaciation, for which the most evidence remains. We highlight key differences between previous interglacials and past periods of rapid climate change from those of today and highlight key areas where future research could fill in knowledge gaps.

### Permafrost history and paleo-extent

Permafrost, ground that remains below 0 °C for at least two consecutive years, forms under cold climate conditions. Permafrost temperatures vary considerably, with colder climates resulting in colder, more extensive, and thicker permafrost. Permafrost typically exists in regions where mean annual air temperatures remain below 0 °C, but permafrost in some regions and at greater depth can exist where mean annual air temperatures are greater than 0 °C. In such instances, permafrost is a relic of a former colder climate that is now protected by peat, overburden, or vegetation<sup>29–31</sup> and is out of equilibrium with modern climate, making it vulnerable to permafrost thaw<sup>32</sup>. While recent increases in permafrost temperatures have been documented across the permafrost zone<sup>21,33</sup> in association with atmospheric warming, past permafrost aggradation is linked to prolonged climatic cooling<sup>34,35</sup>.

The most recent period of widespread permafrost presence in the Arctic likely began after the mid to late Pliocene (3.5–3 Ma) in unglaciated Siberia<sup>36–39</sup>, following a brief (~200,000 year) period of extreme warming centered around 3 Ma known as the mid-Pliocene warm period<sup>40</sup>. The climate cooling that followed coincided with a decline in atmospheric CO<sub>2</sub> concentrations from up to 450 ppm in the early Pliocene (4.5 Ma) to 380 ppm by 2.5 Ma<sup>40</sup>. This cooling led to permafrost aggradation, as evidenced by ice wedge pseudomorphs in northern Yakutia<sup>37,38</sup>, Canada (~3 Ma)<sup>41</sup> and Alaska (~2 Ma)<sup>42,43</sup>, from Pliocene stratigraphic records, and indirectly from pollen at Lake El'gygytyn in Siberia<sup>44</sup>. Permafrost became most expansive within the last million years, with the last culmination between marine isotope stage (MIS) 4 (71–60 ka) to MIS 2–3 (60–18 ka<sup>44–46</sup>) when atmospheric CO<sub>2</sub> levels fell to 220–180 ppm (Figs. 1, 2).

During the Last Glacial Maximum (LGM; 21 ka), permafrost expanded far south of its modern extent<sup>46</sup> (Fig. 1). Field- and model-based reconstructions of the last permafrost maximum suggest a total continuous permafrost-affected region of 26.6–34.5 M km<sup>2</sup> in the northern hemisphere alone<sup>47,48</sup> more than twice as large as the 13.9–18.1 M km<sup>2</sup> directly affected by permafrost today, though the lower modern range is likely underestimating permafrost areas persisting outside of equilibrium with modern climate<sup>47–50</sup>. The biggest losses occurred in Eurasia, which were not compensated by gains made by the recession of the Laurentide Ice Sheet, where sub-ice sheet permafrost likely only persisted under “cold-based” regions of the ice sheet<sup>51</sup>. The contraction of the northern permafrost-affected

landscape by 33–42% (10.8–19.4 M km<sup>2</sup>) since the LGM<sup>47,49</sup> is bound to have had important biogeochemical and climate implications<sup>51</sup>, but the retreat of this extralimital permafrost remains understudied (Fig. 1).

Previous glacial intervals coincided with lower sea levels, exposing continental shelves on which sub-aerial permafrost aggraded in the northern high latitudes. Today, some of this permafrost remains submerged as subsea permafrost and occupies 2–3 M km<sup>2</sup>, primarily in Beringia but also other circumpolar continental shelves<sup>52,53</sup>. At the LGM, in the land that now comprises subsea shelves, permafrost was 20–45% more extensive than subsea permafrost is today (2.5–4.4 M km<sup>2</sup>)<sup>50,52,53</sup>. Post-glacial sea-level rise was substantial (global average: ~15 mm yr<sup>-1</sup>)<sup>54</sup> where isostatic rebound was minimal, resulting in direct flooding of low-gradient, exposed Arctic shelves, some of which were up to 800 km wide in Northeast Siberia and the Bering Sea region<sup>55–57</sup>. Land subsidence resulting from isostatic forebulge collapse likely resulted in rapid inundation of the spatially less expansive Beaufort Sea shelf, whereas uplift of marine sediments in places like Hudson Bay resulted in later permafrost aggradation in the mid to late-Holocene and now contains extensive permafrost peatlands that mostly aggraded in the last 1000 years<sup>34,58</sup>. Subsea permafrost has been gradually thawing since the LGM, but this shelf transgression resulted in partial preservation or even local reformation of permafrost due to cold bottom waters with mean annual temperatures as low as –2 °C on Arctic shelf floors<sup>59</sup>, though shelf bottom water paleotemperatures are not well constrained due to low sedimentation rates. Subsea permafrost is likely most extensive in the nearshore zone<sup>60–62</sup>. Mapping from the Beaufort Sea shelf suggests ice-bearing permafrost extends to the 20 m isobath, which was inundated within the last 5000 years<sup>63</sup>, suggesting that anything deeper would have thawed in the early Holocene if permafrost was present. Multiple studies from the broad Laptev Sea shelf indicate a still widespread presence of ice-bearing subsea permafrost in various stages of preservation<sup>52,64</sup> and geophysical field surveys and numerical modeling of thermal dynamics and salt migration suggest that Holocene thermokarst processes before submergence were priming subsea permafrost in the near-coastal zone towards more rapid degradation following inundation<sup>64,65</sup>.

While permafrost extent contracted on a hemispheric scale during previous interglacial periods, some permafrost persisted throughout these previous warm interglacial intervals, which in part comprises the modern terrestrial permafrost landscape<sup>66–77</sup> (Fig. 1; Supplementary Data 1). Documented extant (present-day) permafrost dating to the warmer-than-present Eemian (130–115 ka; MIS 5e)<sup>67,68,70</sup>, exceptionally warm and wet MIS 11 (424–374 ka<sup>67,68,75</sup>), and as far back as ~650–750 ka<sup>69,71</sup> or even longer<sup>36,77</sup> was found in unglaciated portions of Alaska, Siberia, and Canada (Fig. 1). Notably, these interglacials were warmer than the pre-industrial Holocene<sup>78–80</sup> and encompass a period of substantial collapse of the Greenland and West Antarctic ice sheets ~400 ka<sup>79,80</sup>.

In contrast to northern hemisphere ice sheets, most of which melted away during warm interglacials when ice was in direct contact with the warmer atmosphere, permafrost may have become increasingly protected from warming and thaw at the surface by thickening layers of thawed sediment, peat, and vegetation<sup>29</sup>. Permafrost persistence through these warm interglacials, at least locally, is in part driven by the thermal inertia, latent heat release, and time required to thaw a large mass of frozen, often ice-rich, sediments. The preservation of paleo-active layers in sediments indicates past periods of warming without complete thaw, with cooler subsequent climate conditions refreezing sediments upwards<sup>81</sup>, which could then also lead to the

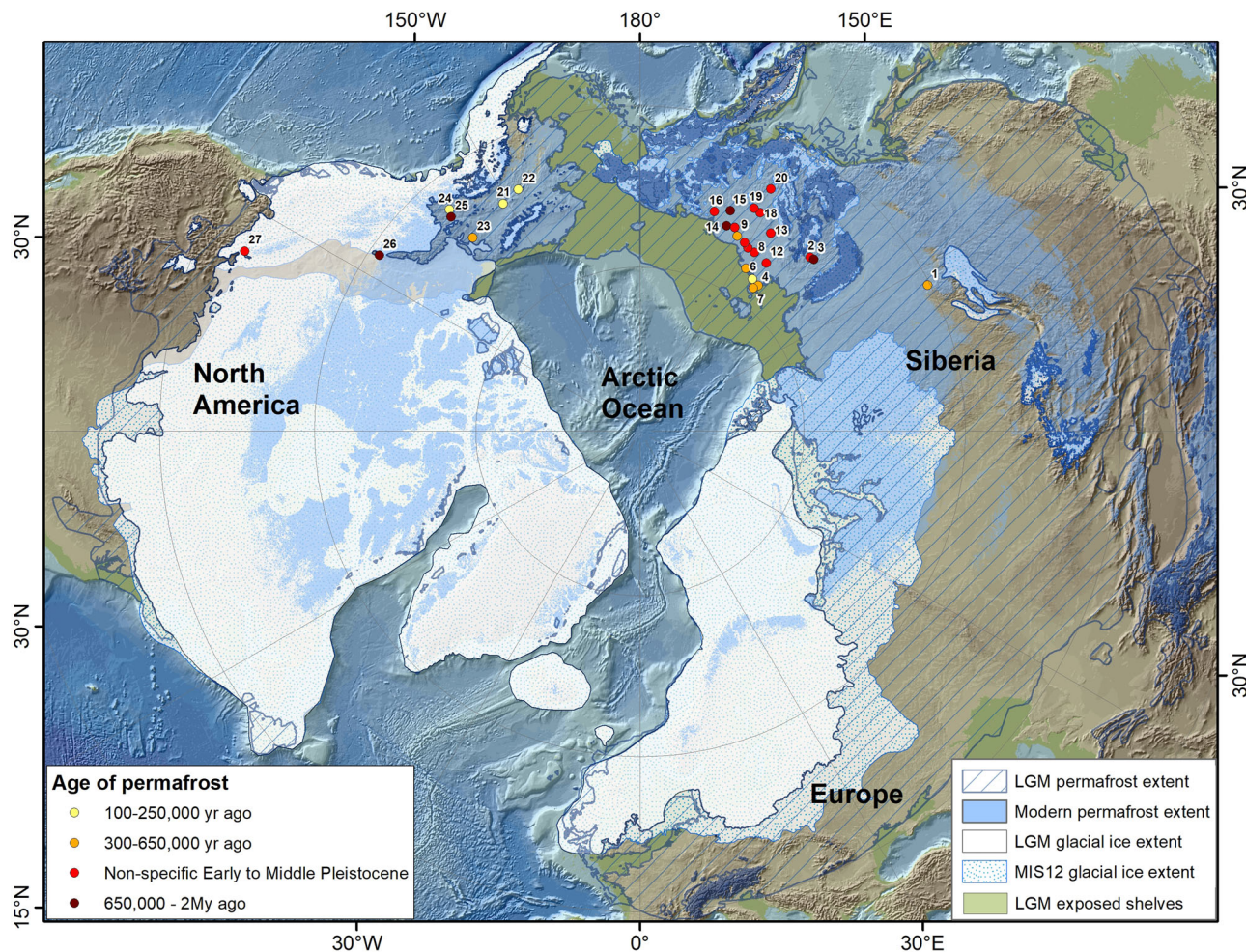


**Fig. 1 Map of modern and last permafrost maximum permafrost region with locations of old extant permafrost.** Modern permafrost<sup>153</sup>, Last Glacial Maximum<sup>154</sup> and MIS12 (477–429 ka) ice sheets, which were among the most extensive of the Pleistocene, are also shown<sup>155</sup>. Locations of ancient permafrost shown in the shaded circles, with colors corresponding to age class of permafrost, falling largely outside of formerly glaciated regions. Numbers refer to the sites in Supplementary Data 1. Map created using ETOPO1 arc-minute global relief model of Earth's surface<sup>147</sup>.

development of secondary or tertiary ice wedges<sup>82</sup>. In addition, the burial of permafrost and other ice by soils and sedimentary overburden helps protect permafrost from top-down thaw on glacial-interglacial time scales. This overburden has also resulted in the survival of glacial ice remnants of the Laurentide ice sheet in Northern Canada<sup>83,84</sup>, the Eurasian ice sheet in Western Siberia<sup>30,85</sup>, and over multiple glacial-interglacial cycles in the New Siberian Islands<sup>86</sup>, until today.

In addition to permafrost aggradation during colder glacial intervals, permafrost aggradation within the current interglacial (the Holocene) was driven by orbital changes that drove a decrease in sunlight reaching northern high latitudes in summer. This led to renewed aggradation of permafrost, including on formerly glaciated land. Enhanced permafrost aggradation after ~3000 years ago until as recently as 150 years ago has been documented from northern peatlands<sup>34</sup>. This relatively young, near-surface permafrost from deglaciated regions is likely much more vulnerable to thaw with sustained warming, given the relative warmth of the permafrost and its proximity to the surface<sup>87</sup>, though to some degree it is protected by the insulative properties of peat<sup>29</sup>.

### Glacial-interglacial permafrost carbon dynamics

**Permafrost aggradation and carbon sequestration.** Permafrost soils and deposits are one of the world's largest terrestrial reservoirs of organic carbon. Permafrost sequesters atmospheric carbon by

halting decomposition of plant and animal remains in the frozen ground, thereby enhancing climate cooling by sequestering atmospheric CO<sub>2</sub> through the accumulation of frozen organic material<sup>88–90</sup>. Thus, the expansion of permafrost area during cold glacial periods increased permafrost OC stocks on land and may have enhanced and sustained glacial climatic cooling. Permafrost carbon accumulated in unglaciated portions of the Arctic during previous Pleistocene glacials, often in extensive permafrost deposits tens of meters thick, such as frozen loess-like Yedoma deposits<sup>42,43,88,89</sup> and loess deposits in Siberia and Europe outside of the modern permafrost<sup>46</sup> (Fig. 3; Supplementary Data 2). Permafrost formation during and prior to the LGM also preserved some peat deposits from the previous interglacial, although the size of this C stock is unknown. During the Holocene, additional carbon was incorporated into permafrost as permafrost formed on formerly glaciated landscapes<sup>34</sup>. In total, it is estimated that present-day near-surface (upper ~3 m) permafrost beneath exposed land surfaces contains nearly ~1015–1035 Pg C of Holocene and late-Pleistocene age<sup>1,2</sup>, with an additional 624–869 Pg C in depths >3 m<sup>51</sup> up to a million years old<sup>77</sup> (Fig. 3; Supplementary Data 1, 2), representing a major present-day reservoir of carbon.

**Permafrost thaw and carbon remobilization.** Permafrost thaw occurs when ground temperatures exceed the freezing point, leading to remobilization of formerly frozen soil carbon.

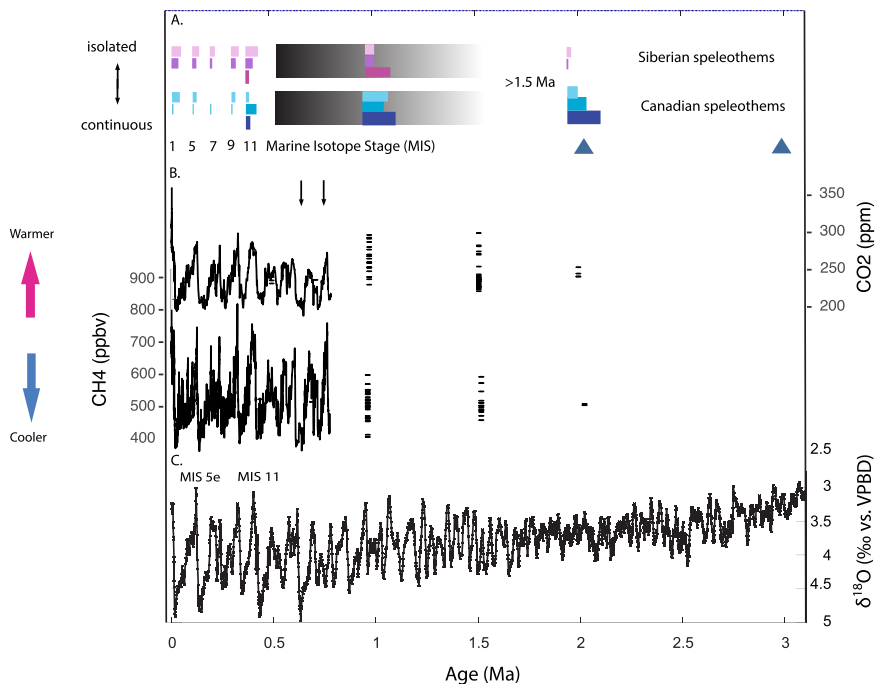


**Fig. 2** Permafrost evolution over the last 3 million years. **A** Data shown are the Siberian<sup>67</sup> and Canadian<sup>68</sup> speleothem records of thaw from the continuous (dark pink and blue, respectively), discontinuous (medium purple and blue, respectively), and sporadic (light pink and blue, respectively), with gray bars indicating likely aggradation of northern permafrost ~1.3 Ma. Blue triangles indicate the timing of ice wedge casts from Alaska and Canada that suggest previous permafrost presence, and black arrows indicate the oldest extant permafrost from Batagay megaslump, Siberia (~650 ka)<sup>75</sup> and Canada (~750 ka)<sup>71</sup>. **B** Antarctic ice core carbon dioxide and methane measurements<sup>156,157</sup> **C** LR04 deep-sea oxygen isotope stack<sup>158</sup>.

Permafrost soils can thaw gradually through active layer thickening, or in the case of ice-rich permafrost, they can thaw several meters at once (abrupt thaw; years to decades), forming thermokarst lakes, collapse-scar wetlands, and causing hillslope erosion<sup>91</sup>. Permafrost carbon can also be remobilized as dissolved and particulate forms of OC to downstream watersheds, coastal zones, and ocean sediments. Evidence of paleo-permafrost thaw is recorded in proxies such as basal dating of thermokarst lake formation<sup>92,93</sup>, abrupt transitions in peat cores<sup>94,95</sup>, and biomarkers of terrestrial carbon in coastal ocean cores<sup>96–100</sup>. Evidence for extensive LGM permafrost thaw exists for the last glacial termination (~18–10 ka), when abrupt warming led to massive OC remobilization from the terrestrial landscape to the ocean and atmosphere<sup>92,96–100</sup>. Rapid warming during the Bølling-Allerød (14.7–12.8 ka) and Younger Dryas-Preboreal transition (11.7–~10 ka) shows evidence of some of the highest rates of thermokarst and thaw lake development in yedoma regions of Alaska and Siberia of the entire interglacial, including today<sup>92,93</sup> (Fig. 4), consistent with other field evidence for elevated remobilization of permafrost carbon into lakes<sup>101</sup> and through fluvial systems<sup>102</sup> into marine sediments<sup>96–100</sup>. Deglaciation of massive ice sheets uncovered ~120–157 Pg C<sup>51,103</sup> that was buried under cold portions of the ice sheets<sup>51</sup>.

*Carbon stored in thawed ice-rich landforms and former and new permafrost landscapes.* Warming during the last deglaciation also triggered organic carbon sequestration in northern regions in the form of vegetation, cryoturbated soils, lake sediments, and peat<sup>104,105</sup>. Deglacial thermokarst lake formation across vast regions of Alaska and Siberia recovered carbon lost to the atmosphere from permafrost thaw through lake sediment and peat accumulation in drained lake basins<sup>104,105</sup>. By 5000 years ago, pan-Arctic thermokarst lakes transitioned from carbon sources to carbon sinks, ultimately increasing the carbon pool in the region by over 50 percent compared to previous estimates<sup>104</sup>.

Vast newly deglaciated or uplifted landscapes across northern Canada and northern Europe also aggraded permafrost in the Holocene, and permafrost aggradation in peatlands in the late Holocene<sup>34</sup> increased the 'inert' carbon pool to  $185 \pm 66$  Pg C by present day<sup>51</sup>, not including 410 Pg C in global buried peat deposits<sup>106</sup>. The contribution of thermokarst lakes to the removal of carbon from the atmosphere contributed to atmospheric cooling of  $0.06 \text{ W m}^{-2}$  by the pre-industrial<sup>104</sup>. Today, thermokarst-impacted landscapes store proportionally larger pools of permafrost carbon than other non-thermokarst landscapes<sup>107</sup>. Some estimates suggest that the total carbon pool of the permafrost region has increased since the LGM<sup>51,104</sup>, though estimates of by how much remain highly uncertain. While the "inert" permafrost carbon pool is ~37% less than during the LGM<sup>51</sup>, this is partially offset by net carbon gains in permafrost and former permafrost landscapes<sup>51,104,107</sup> and can be attributed in part to aggradation of carbon-rich permafrost in deglaciated landscapes and in now permafrost-free landscapes<sup>51</sup>. The net carbon balance of the permafrost region over glacial and interglacial time scales remains an open question.

#### Assessing past evidence for permafrost destabilization and rapid carbon release

Abrupt climate transitions, such as at the end of the Younger Dryas (11.7 ka) (Fig. 4), coincide with rapid increases in greenhouse gas concentrations. Ice core records show a doubling of CH<sub>4</sub> concentrations at the end of the YD in a matter of decades to centuries coupled with a warming of ~2 °C<sup>108</sup>, but the extent to which permafrost carbon rapidly thawed, mineralized, and contributed to the rise in atmospheric methane concentrations (AMC)<sup>11–13,109,110</sup>, and atmospheric CO<sub>2</sub><sup>97,111,112</sup> remains debated. Because carbon is lost from permafrost at a rate faster than post-thaw uptake<sup>94</sup>, release from thawing permafrost as CO<sub>2</sub> and CH<sub>4</sub> should be recorded in the paleo record of the

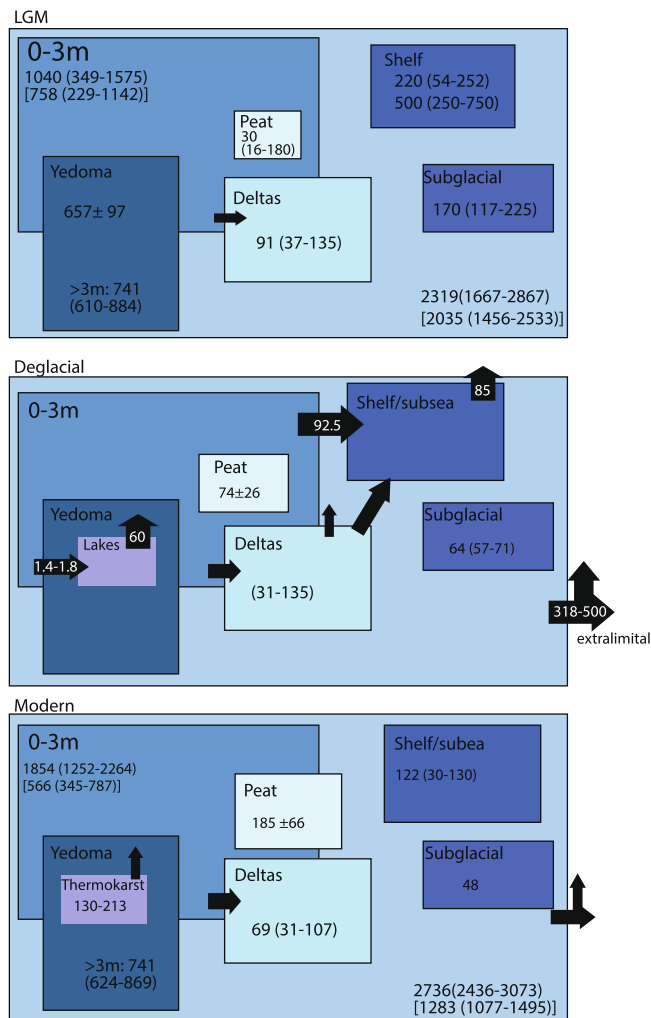


**Fig. 3 Carbon stocks (Pg C) for the LGM and present-day and stocks and fluxes for the deglacial period defined here as 14.7–8 ka.** Values taken primarily from ref. <sup>51</sup>, with additional values for Yedoma from ref. <sup>45</sup> and subglacial from ref. <sup>103</sup>, and subsea from <sup>53</sup>. Extralimital are from refs. <sup>51,89</sup>.

atmosphere, providing potential insights into the future permafrost carbon climate feedback. Air bubbles in ice cores are trapped archives of paleo-atmospheres that record changes in concentrations and isotopic composition of greenhouse gases with time. Here, we explore evidence suggesting extensive permafrost thaw during previous deglaciations led to mineralization of large quantities of permafrost OC, which over subsequent millennia, was recovered into permafrost deposits.

The frequency of thermokarst lake initiation and bottom-up calculations of their methane emissions contributed to a peak of  $16.8 \text{ Tg yr}^{-1}$ <sup>104</sup> over centennial and millennial timescales of the last deglaciation (Fig. 4). Peak lake formation, however, is offset from the decadal-scale doubling of AMC by  $\sim 1000$  years and the landscape-scale formation of lakes was more gradual than the AMC rise<sup>93,110</sup>, suggesting other processes contributed to northern hemisphere sources of rapid AMC rise (globally, much of the AMC rise originated in the tropics<sup>113,114</sup>). The bottom-up emissions estimates from thermokarst lakes are roughly consistent with top-down isotope constraints from ice cores ( $<15.4\text{--}19 \text{ Tg CH}_4 \text{ yr}^{-1}$ )<sup>11–13</sup> on permafrost OC sources. The agreement in these estimates suggests that the bottom-up contributions from thermokarst lakes comprise nearly all the permafrost carbon emissions allowed by the constraints of the top-

down models<sup>13</sup>, which assume an upper limit based on the  $^{14}\text{C}$  constraint of “old” carbon ( $^{14}\text{C}$ -depleted) from permafrost<sup>11,13</sup>.

Two sources of uncertainty are the misconception about the age of permafrost OC upon thaw and the lack of understanding of the role of extralimital permafrost. The mixing between older, newly thawed permafrost OC sediments and recently fixed OC in thermokarst lakes and wetlands can produce a younger  $\text{CO}_2$  and  $\text{CH}_4$  emissions signal<sup>115,116</sup>, confounding modeling assumptions about permafrost OC age, which could increase the upper limit on permafrost thaw contributions to deglacial AMC<sup>110</sup>. Furthermore, permafrost existed on broad continental shelves ( $3.5 \text{ M km}^2$ )<sup>53</sup> and in regions within the last permafrost maximum to the south of modern permafrost extent during the LGM; this covered an additional  $\sim 12\text{--}20 \text{ M km}^2$ <sup>50</sup> and likely included relatively younger permafrost. Other likely sources of  $\text{CH}_4$  from thawing permafrost during deglaciation include subglacial permafrost<sup>103</sup> and, likely to a lesser extent, thaw in peatlands. However, key information on factors like pre-thaw carbon stocks, ice content, and the timing and rates of permafrost thaw from these extralimital regions remain unknown. Emissions from this large region could push the pulse of permafrost thaw derived  $\text{CH}_4$  and  $\text{CO}_2$  contributions earlier. We conclude that the emissions contributions of newly thawed permafrost carbon in deglacial atmospheric  $\text{CH}_4$  records remains an open question that requires further exploration. Regardless, numerous lines of evidence, including isotopic constraints, suggest catastrophic  $\text{CH}_4$  hydrate release, beneath  $>200 \text{ m}$  deep permafrost or under significant pressure from overlying ocean, to the atmosphere did not occur during past Pleistocene warming events and is thought to be unlikely to occur in the near future<sup>11–13,110,111,113,114</sup>.

The contribution of permafrost carbon to the rise of atmospheric  $\text{CO}_2$  concentrations during deglaciation remains less constrained than  $\text{CH}_4$ , despite carbon release from permafrost thaw being predominantly in the form of  $\text{CO}_2$ <sup>117</sup>. Nevertheless, changes in both stable and radioactive isotopes of  $\text{CO}_2$ , particularly during a period in early deglacial (17.5–14.5 ka) known as the “Mystery Interval”, when  $\Delta^{14}\text{C}$  concentrations changed significantly and  $\delta^{13}\text{C}\text{-CO}_2$  decreased by  $0.4\text{‰}$ <sup>118</sup> that was accompanied by a rise in  $\text{CO}_2$  by 35 ppm, have been attributed in part to the release of old carbon from thawing permafrost<sup>97,111,112</sup> (Fig. 4), particularly for centennial-scale shifts that cannot be easily explained by ocean processes<sup>97,111,112</sup> that overwhelmingly influence changes in pre-industrial atmospheric  $\text{CO}_2$  concentrations<sup>119</sup>. Limited evidence from terrestrial biomarkers in ocean cores suggests that deglacial permafrost thaw, through sea-level rise and flooding of Arctic shelves, could have released 85 Pg C, which in part could explain the changes in atmospheric  $\text{CO}_2$   $\sim 14.5 \text{ ka}$  ( $12 \pm 1 \text{ ppm}$ ) and  $11.5 \text{ ka}$ <sup>97</sup> (Fig. 4).

Looking further back in time, little evidence exists in the ice core record for enhanced permafrost carbon-climate feedbacks with greater warming during previous warm and wet ‘super-interglacials’. Examination of  $\text{CO}_2$  and  $\text{CH}_4$  concentrations from past warmer-than-pre-industrial interglacials, such as MIS 5e and MIS 11 (Fig. 2), does not show concentrations above Holocene levels, suggesting that permafrost thaw contributions of  $\text{CO}_2$  and  $\text{CH}_4$  concentrations did not exceed those of the current interglacial. However, it is also possible that past carbon release happened gradually enough to be buffered by the ocean<sup>68</sup> and by the terrestrial biosphere, such as through the atmospheric C uptake by the formation of peatlands and soils on newly unglaciated landscapes<sup>34</sup>. Permafrost carbon stocks for previous interglacials remain unconstrained, and the quality and temporal resolution of the greenhouse gas concentrations from ice cores are not sufficient to resolve decadal-scale variations as during the last deglaciation.

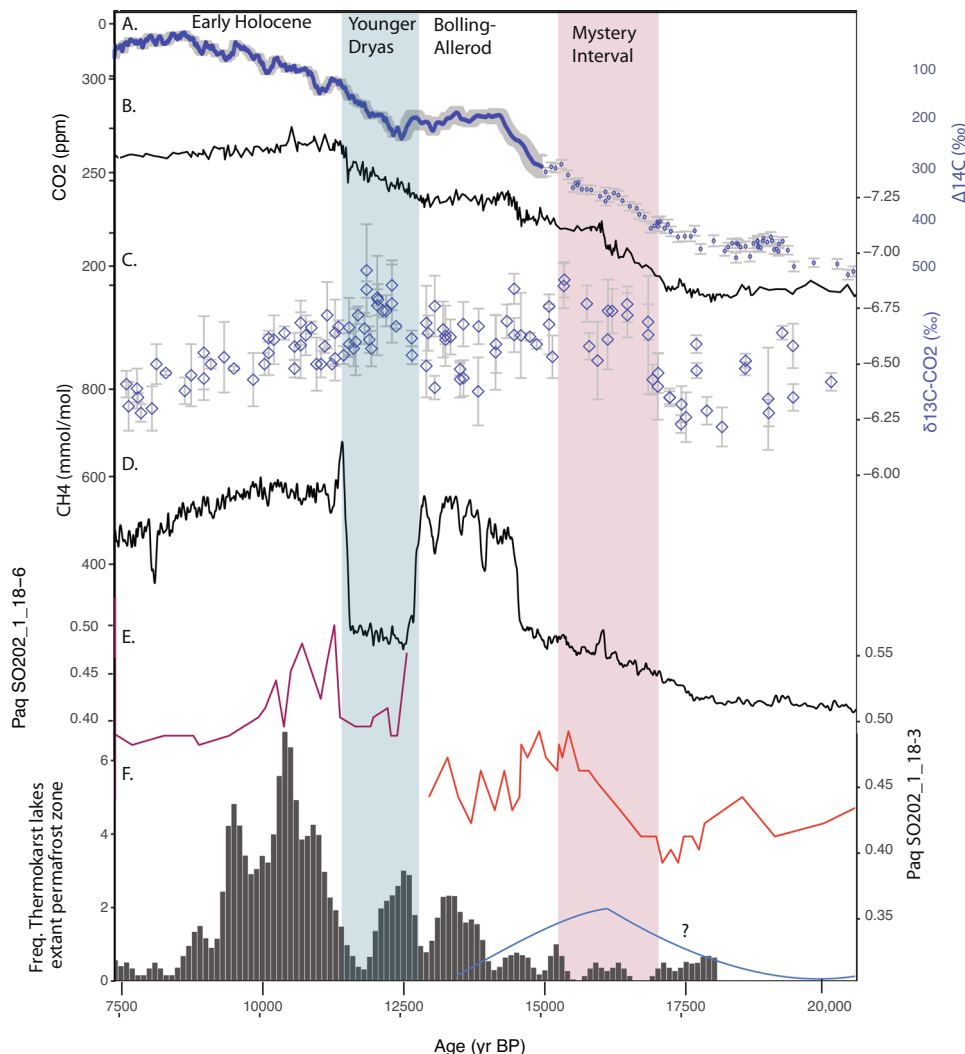


**Fig. 4 Deglacial atmospheric composition of the atmosphere and proxies for permafrost thaw.** **A** Radiocarbon content of the atmosphere with standard deviations<sup>159</sup>; **B** Atmospheric CO<sub>2</sub> concentrations<sup>160</sup>; **C** EDC96 δ<sup>13</sup>C-CO<sub>2</sub> with standard deviations<sup>161</sup>; **D** Atmospheric CH<sub>4</sub> concentrations<sup>160</sup>; **E** Paq, a proxy for the ratio of wetland to terrestrial plants, which is used as an indicator of permafrost thaw from shelf regions, for two cores in the North Pacific<sup>99</sup>; **F** Frequency of thermokarst lakes<sup>93</sup> from the extant permafrost zone (gray bars) and the hypothesized contribution from extralimital permafrost (blue curve).

### Landscape considerations with permafrost susceptibility to thaw

Using the past to inform the future can be useful, but key differences in starting conditions prior to abrupt warming events in the past will likely elicit a different response to future warming. On the one hand, we argue that landscape differences in geomorphology, ground ice content, sea level, and glacial extent make permafrost less susceptible to thaw today than during the last deglaciation, implying a higher threshold response is necessary to achieve the same degree of widespread and rapid permafrost thaw. On the other hand, the modern landscape may be less primed for carbon recovery than the newly deglaciated landscapes of glacial terminations. In the past, ice-rich landscapes showed high direct sensitivity to atmospheric warming<sup>120,121</sup>, likely similar to the rapid thaw of cold, ice-rich permafrost with little protection by insulating layers in the high Arctic tundra today<sup>23,25,122,123</sup>. However, these ice-rich, poorly vegetated landscapes are likely less spatially extensive today than at the last deglaciation<sup>101</sup>. In the modern permafrost environment, lower near-surface ground ice content due to the presence of deeper paleo-active layers from the Holocene Thermal Maximum<sup>124</sup>,

greater insulative effects of peat and vegetation<sup>29,101</sup>, and a geomorphologically more matured landscape (e.g., thaw of most near-surface ice-rich Yedoma since the LGM)<sup>101,125</sup> contribute to the slower responsiveness to warming of today's permafrost. In addition, the hydrological network in permafrost landscapes has evolved over the Holocene, limiting thermokarst lake initiation and growth to less extensive geomorphologically suitable areas than during the deglacial period<sup>101,125</sup>. Together, these factors may explain why observed rates of new thermokarst lake development and carbon remobilization are lower today than in the past<sup>101,102</sup>, suggesting present-day warming has not yet caused the widespread level of permafrost thaw experienced during early deglaciation, despite amplified Arctic warmth.

**Differences in climate sensitivity of permafrost carbon.** The higher sensitivity of permafrost carbon remobilization during the last deglaciation compared to today is evident when calculating the carbon flux per °C, which shows much higher sensitivity during deglaciation than modern permafrost carbon losses and some scenarios into the future<sup>91,126</sup> (Supplementary Data 3). Measurements of permafrost carbon flux, particularly those with

well constrained timing, are lacking for the deglacial, with the exception of thermokarst lakes<sup>104,110</sup>. Methane fluxes from modern thermokarst lakes are less than half than fluxes calculated from early Holocene thermokarst lakes<sup>93,104</sup>. The CH<sub>4</sub> feedback of thermokarst lakes during parts of the deglacial were as high as 10.5 Pg C per °C, which is an order of magnitude higher than that of today (0.15–0.19 Pg C per °C) and double the projected feedback from all abrupt thaw (including thermokarst lake, hillslope erosion, peatland thaw) under RCP 4.5 by 2300<sup>91</sup> (Supplementary Data 3). While the contribution from peatland thaw would have been markedly less during deglaciation, hillslope erosion would have likely been as high or higher than today<sup>121</sup>. Similarly, contribution from deglacial inundation of shelf regions yielded a release of 9.4 Pg C per °C, assuming release of the published 85 Pg C occurred between 16–8 ka<sup>97</sup> (Supplementary Data 3), but the timescale of these fluxes is not well constrained, making this value highly uncertain. Nevertheless, these findings indicate that sensitivity of carbon release from permafrost thaw was greater during past abrupt warming events, which may point to the influence of landscape history as a potential mechanism to explain these differences but could suggest limitations to the linear framework used to explain warming from these processes.

*Landscape-level post-thaw carbon uptake differences.* Key differences in landscape properties between the end of the last ice age and today may limit future uptake of carbon at the same scale. At the circumarctic scale, the deglacial retreat of ice sheets gave way to the expansion of carbon-rich ecosystems, including peatlands and glacial lakes (Fig. 4). The carbon stocks in northern peatlands increased by 330 Pg during this interglacial period, as peatlands expanded across the newly deglaciated landscape, and peat accumulated in drained thermokarst lake basins and other water bodies<sup>101,104,105</sup> (Figs. 3, 5). Warming and wetting climate also allowed for peat initiation on unglaciated landscapes in the Arctic<sup>121,127,128</sup>. The expansive newly deglaciated land area allowed for the proliferation of these carbon-rich ecosystems and climatic cooling increased permafrost aggradation in peatlands in the late Holocene<sup>34</sup>, increasing the carbon pool in the northern permafrost region by 400 Pg over multiple millennia, despite a decrease of ~700 Pg of permafrost carbon over the same period<sup>51</sup>. However, apart from the centennial to millennial time scale required for new peat accumulation, future carbon sequestration by peat formation may be limited by the relatively small areas of newly deglaciated land and the climate and land-use driven potential loss of peatland carbon sinks at the southern margins of their current extent<sup>106,129</sup>. New glacial lake formation is limited by the smaller spatial extent of modern ice sheet area and comparatively lower near-surface massive ground ice extent than the deglacial period<sup>93,130</sup>. Although massive Holocene ice wedges mostly are smaller than those of the Pleistocene<sup>125,130,131</sup>, segregated ice in organic-rich fine-grained deposits can still contribute to ponding associated with thermokarst<sup>132</sup>. The Arctic landscape today may be less primed for carbon recovery through establishment of carbon-rich ecosystems because of the difference in spatial and geomorphic landscape configuration today and the speed at which the climate is changing compared to the geologic record. Unlike regional permafrost thaw between the end of the LGM and the pre-industrial era, permafrost that thaws today is unlikely to re-aggrade in most places due to today's warming climate. The fate of existing near-surface permafrost will depend largely on emissions reduction targets that limit warming below 2 °C, but temperature anomalies in parts of the Arctic have already exceeded 5 °C<sup>133</sup> and may exceed 10 °C under RCP8.5 by end of the 21st century<sup>16</sup>, with additional vulnerability driven by changing fire and precipitation regimes<sup>134,135</sup>.

The rate and timescale of carbon sequestration compared to loss in these permafrost landscapes is an important consideration for the permafrost carbon-climate feedback. Contemporary evidence from thermokarst lakes and thawing permafrost peatlands shows the release of an initial pulse of carbon to the atmosphere as CO<sub>2</sub> and CH<sub>4</sub> in the decades immediately after thaw, followed by slow accumulation of carbon in lake sediments and peat through new biological productivity in thawed landscapes<sup>94,95,105,107</sup>. While the carbon losses from thawing permafrost occur on the order of decades, the recovery of this ecosystem carbon pool can take centuries to millennia<sup>94,95</sup>. This carbon recovery could return these landscapes to net carbon sinks with a negative radiative forcing that would cool the climate, but the timescales are too long to be included in anthropogenic climate mitigation strategies.

The sources of the greatest uncertainty in both the modern and paleo record are subsea permafrost and the storage of CH<sub>4</sub> in and under permafrost acting as a cap that can potentially be released through gas emission craters, taliks, or faults. Recent measurements on the Siberian shelf document CH<sub>4</sub> saturation and ebullition from the East Siberian Arctic Shelf<sup>136–139</sup> and have been found to be largely derived from thermogenic sources<sup>137</sup>; however, it remains unclear if the rate of modern observed fluxes differs significantly from long-term Holocene average fluxes, given the slow response of subsea permafrost that is buffered by cold bottom waters to thaw. Questions remain about how the permafrost-carbon feedback will play out as high-latitude temperatures begin to exceed those of previous warm Pleistocene interglacials or the most recent deglaciation, but data so far do not support significant geologic emissions derived from arctic shelves or subsea permafrost<sup>11,114</sup>, as warmer bottom waters will facilitate enhanced thaw of relatively warm, isothermal subsea permafrost<sup>138</sup>.

The recent discovery of blow-out craters in Siberia also points to a previously uncharacterized process in the paleorecord. These craters are thought to form from a buildup in pressure of CH<sub>4</sub> gases within the permafrost that ultimately erupt to the surface. While their formation remains debated, they may be facilitated in part by infiltration of water into cracks in the permafrost and associated talik formation, further fueled by microbial and thermogenic gasses emanating from faults and fractures in the underlying bedrock that cause a build-up of gases that eventually erupt through the surface<sup>140,141</sup>. Terrestrial CH<sub>4</sub> super-seeps releasing <sup>14</sup>C-depleted or fossil CH<sub>4</sub> have been documented in NW Canada, Russia, and Alaska<sup>140,142,143</sup>, including the largest known super seep emitting fossil coalbed CH<sub>4</sub> in a lake northwest Alaska<sup>143</sup>; however, their total present day emission in the Arctic is not large (~2 Tg CH<sub>4</sub> yr<sup>-1</sup>) (148). Given isotopic constraints on AMC in the ice core record<sup>11–13</sup>, these fossil carbon sources were likely relatively unimportant contributors to the rise in atmospheric CH<sub>4</sub> in the paleorecord<sup>11–13</sup>. However, release of deep, thermogenic CH<sub>4</sub> cannot be ruled out as a contributor under future climate change as surface permafrost warms and continues to degrade. Determining the timing of super-seep formation and its relationship to permafrost dynamics will also aid future projections of permafrost climate feedbacks.

Mounting evidence exists that permafrost thaw is accelerating above rates observed over millennia, as an unprecedented rate and degree of warming, driven by an increase in greenhouse gas concentrations not observed at any time during the Pleistocene Ice Age of the last 2.6 M years, could soon push the northern permafrost region into a period of intensified thaw that is unprecedented over this period. Half to 140% of the 6 °C global warming that occurred over 8,000 years from 18 ka to 10 ka<sup>108,144</sup> is now projected to occur in the Arctic within 80 years by 2100 under the RCP 8.5 emission scenario<sup>14</sup>. Locally, permafrost that has

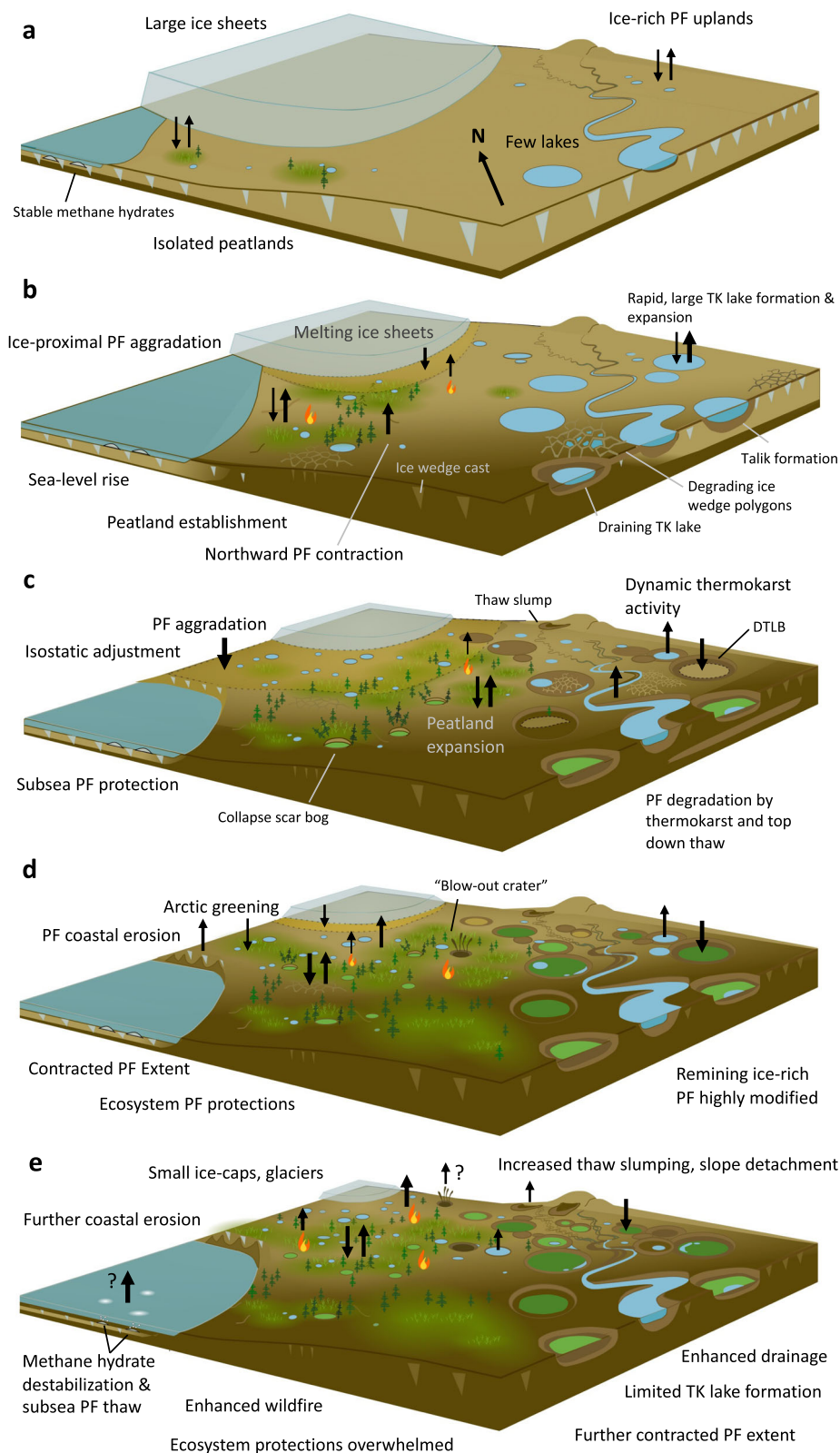


**Fig. 5 Landscape comparison across multiple timescales, showing permafrost (PF) and thermokarst (TK) changes through deglaciation.** **a** Late glacial (~20–14 ka) landscape, **b** deglacial and early Holocene (~14–8 ka), **c** mid- to late- Holocene (~8–1 ka), **d** modern day, **e** warmer future. Arrows indicate changes in carbon storage for various pools in the Arctic landscape, with arrow weight indicating size of flux. Upward facing arrows indicate net flux from permafrost deposits and downward facing arrows indicate net flux to permafrost deposits. In some instances, landforms can be initial large emitters of CH<sub>4</sub> but an overall small net carbon sink (e.g., collapse-scar bogs). DTLB drained thermokarst lake basins. Figure is not to scale and some features appear closer together or to the surface for illustrative purposes (e.g., methane hydrates occur >200 m depth).

**Table 1 Key concepts contextualizing permafrost carbon dynamics on geologic timescales.**

	<b>Extent</b>	<b>Thaw</b>	<b>Carbon loss</b>	<b>Carbon gain</b>
Paleo-permafrost (glacials)	Expanded beyond modern extent during glacials	Low rates of thaw	Minimal carbon remobilization	Accumulated slowly in unglaciated regions; persistence of permafrost beneath 'cold-based' ice sheets
Paleo-permafrost (interglacials)	Contracted during interglacials, but some survived interglacials warmer than today	High rates of thaw during deglaciation; methane hydrates remained stable	High rates of carbon remobilization; evidence for some of the atmospheric rises CH <sub>4</sub> and CO <sub>2</sub> (particularly decadal to centennial shifts not easily explained by ocean processes), but permafrost was not the primary driver of these increases; high remobilization and redeposition into waterbodies; carbon loss from extralimital areas remains poorly constrained	Permafrost carbon losses offset by soil carbon gains through peat and lake sediment accumulation and carbon-rich ecosystems expanding over newly deglaciated landscapes, but net cooling is realized over centennial to multi-millennial timescales
Modern Permafrost	Modern extent ~33–42% of permafrost extent at the Last Glacial Maximum	Higher permafrost thaw threshold than deglaciation due to ecosystem protection	Moderate rates of carbon remobilization, minimally responsible for rise in atmospheric CH <sub>4</sub> and CO <sub>2</sub> ; Permafrost carbon is ~63% of that at LGM	Carbon loss from near-surface permafrost thaw leading to some recovery through net primary productivity and rapid post-thaw peat accumulation
Future permafrost	Significantly reduced in the near surface (<3 m), with some surviving at depth	Greater permafrost thaw rates rivaling deglaciation due to crossing temperature threshold to warm ground: potential for release of sub-permafrost methane hydrates over millennial time scales.	High rates of carbon remobilization that will enhance the carbon-climate feedback, but not the primary driver	Future landscapes less primed for carbon recovery than deglaciation because of a lack of deglaciated land area, ecosystem disturbances, and landscape geomorphology

survived for at least 400,000 years is beginning to thaw<sup>67</sup>, and Arctic amplification that will only increase with decreasing sea ice extent is expected to enhance permafrost thaw<sup>72,145,146</sup>. Recent extended heat waves north of the Arctic circle, along with substantial fire disturbance<sup>134</sup>, globally rising permafrost temperatures<sup>21</sup>, and accelerating rates of thaw and erosion<sup>146</sup>, suggest that permafrost extent is currently in a state of rapid change<sup>19,23,24,64</sup>, and massive as well as excess segregated ground ice makes permafrost susceptible to rapid thaw even in deeper deposits<sup>147</sup>. Some local areas are experiencing exceedingly high rates of lake formation and expansion due to warming since the 1980s<sup>27</sup>. As the rate of sea-level rise now accelerates<sup>148</sup> and sea ice declines<sup>145,149</sup> low-lying areas become inundated, amplifying coastal erosion, which dominates Arctic permafrost coastal processes today<sup>150</sup>. Some of the carbon mobilized is buried in marine sediments<sup>151</sup>, but a fraction is released to the atmosphere<sup>136,139,152</sup>.

## Conclusions

This review identifies landscape considerations and compares rates of change that impact permafrost carbon dynamics through periods of rapid climate change. Key points are summarized in Table 1. We also highlight areas of research that could help further constrain permafrost carbon dynamics through periods of past climate change that could provide important information for the future. These include better constraints on subsea permafrost extent and its carbon pool, as well as understanding of the response to warming bottom waters and stability of subsea CH<sub>4</sub> hydrates, particularly in the nearshore environment. As terrestrial permafrost continues to thaw and as climate warming is poised to exceed the rates of change of Pleistocene glacial-interglacial cycles, more research is needed on the stability of terrestrial gas hydrates, which are currently capped by thick permafrost. Further constraints on CH<sub>4</sub> and CO<sub>2</sub> dynamics from a range of permafrost thaw process, including talik (unfrozen ground in permafrost) growth, blow-out crater formation, terrestrial gas hydrate dissociation, thermo-erosion, and coastal erosion are needed to quantify movement and deposition of carbon among various pools (soils, lakes, ocean, and atmosphere), and sequestration processes, particularly of terrestrial carbon in the marine environment. Multiple lines of evidence suggest that the modern extent of thaw has not yet exceeded that of the last deglaciation, but the potential for a stronger permafrost carbon-climate feedback to ongoing and future Arctic climate warming remains a possibility for this century.

## Data availability

Supplementary Data Tables 1–3 are available at the figshare database <https://doi.org/10.6084/m9.figshare.23279855.v1>.

Received: 27 January 2023; Accepted: 12 June 2023;

Published online: 25 July 2023

## References

- Mishra, U. et al. Spatial heterogeneity and environmental predictors of permafrost region soil organic carbon stocks. *Sci. Adv.* **7**, eaaz5236 (2021).
- Schuur, E. A. et al. Climate change and the permafrost carbon feedback. *Nature* **520**, 171–179 (2015).
- Friedlingstein, P. et al. Global carbon budget 2020. *Earth Syst. Sci. Data* **12**, 3269–3340 (2020).
- Mascarelli, A. A sleeping giant? *Nat. Clim. Change* **1**, 46–49 (2009).
- Brown, A. Pandora's freezer? *Nat. Clim. Change* **3**, 442–442 (2013).
- Treat, C. C. & Frohling, S. A permafrost carbon bomb? *Nat. Clim. Change* **3**, 865–867 (2013).
- Brouillette, M. How microbes in permafrost could trigger a massive carbon bomb. *Nature* **591**, 360–363 (2021).
- Lenton, T. M. et al. Tipping elements in the Earth's climate system. *Proc. Natl. Acad. Sci.* **105**, 1786–1793 (2008).
- Lenton, T. M. et al. Climate tipping points—too risky to bet against. *Nature* **575**, 592–595 (2019).
- Armstrong McKay, D. I. et al. Exceeding 1.5 C global warming could trigger multiple climate tipping points. *Science* **377**, eabn7950 (2022).
- Petrenko, V. V. et al. Minimal geological methane emissions during the Younger Dryas–Preboreal abrupt warming event. *Nature* **548**, 443–446 (2017).
- Petrenko, V. V. et al. 14CH<sub>4</sub> measurements in Greenland ice: investigating last glacial termination CH<sub>4</sub> sources. *Science* **324**, 506–508 (2009).
- Dyonisius, M. N. et al. Old carbon reservoirs were not important in the deglacial methane budget. *Science* **367**, 907–910 (2020).
- Tierney, J. E. et al. Past climates inform our future. *Science* **370**, eaay3701 (2020).
- Turetsky, M. R. et al. Permafrost collapse is accelerating carbon release. *Nature* **569**, 32–34 (2019).
- Canadell, J. G. et al. Global carbon and other biogeochemical cycles and feedbacks. (2021).
- Schuur, E. A. et al. Permafrost and climate change: carbon cycle feedbacks from the warming Arctic. *Annu. Rev. Environ. Resour.* **47**, 343–371 (2022).
- Natali, S. M. et al. Incorporating permafrost into climate mitigation and adaptation policy. *Environ. Res. Lett.* **17**, 091001 (2022).
- Liljedahl, A. K. et al. Pan-Arctic ice-wedge degradation in warming permafrost and its influence on tundra hydrology. *Nat. Geosci.* **9**, 312–318 (2016).
- Kokelj, S. V., Lantz, T. C., Tunnicliffe, J., Segal, R. & Lacelle, D. Climate-driven thaw of permafrost preserved glacial landscapes, northwestern Canada. *Geology* **45**, 371–374 (2017).
- Biskaborn, B. K. et al. Permafrost is warming at a global scale. *Nat. Commun.* **10**, 264 (2019).
- Nitze, L., Grosse, G., Jones, B. M., Romanovsky, V. E. & Boike, J. Remote sensing quantifies widespread abundance of permafrost region disturbances across the Arctic and Subarctic. *Nat. Commun.* **9**, 5423 (2018).
- Farquharson, L. M. et al. Climate change drives widespread and rapid thermokarst development in very cold permafrost in the Canadian High Arctic. *Geophys. Res. Lett.* **46**, 6681–6689 (2019).
- Lewkowicz, A. G. & Way, R. G. Extremes of summer climate trigger thousands of thermokarst landslides in a High Arctic environment. *Nat. Commun.* **10**, 1329 (2019).
- Nitzbon, J. et al. Fast response of cold ice-rich permafrost in northeast Siberia to a warming climate. *Nat. Commun.* **11**, 2201 (2020).
- Vasiliev, A. A. et al. Permafrost degradation in the western Russian arctic. *Environ. Res. Lett.* **15**, 045001 (2020).
- Anthony, K. W. et al. Decadal-scale hotspot methane ebullition within lakes following abrupt permafrost thaw. *Environ. Res. Lett.* **16**, 035010 (2021).
- Alley, R. B. et al. Abrupt climate change. *Science* **299**, 2005–2010 (2003).
- Shur, Y. L. & Jorgenson, M. T. Patterns of permafrost formation and degradation in relation to climate and ecosystems. *Permafrost Periglacial Process.* **18**, 7–19 (2007).
- Astakhov, V. I. & Isayeva, L. L. The 'Ice Hill': an example of 'retarded deglaciation' in Siberia. *Quat. Sci. Rev.* **7**, 29–40 (1988).
- Ananjeva, G. V., Melnikov, E. S. & Ponomareva, O. E. Relict permafrost in the central part of Western Siberia. in *Proceedings of the 8th International Conference on Permafrost* 1, 2003–2005 (2003).
- Chadburn, S. E. et al. An observation-based constraint on permafrost loss as a function of global warming. *Nat. Clim. Change* **7**, 340–344 (2017).
- Smith, S. L., O'Neill, H. B., Isaksen, K., Noetzli, J. & Romanovsky, V. E. The changing thermal state of permafrost. *Nat. Rev. Earth Environ.* **3**, 10–23 (2022).
- Treat, C. C. & Jones, M. C. Near-surface permafrost aggradation in Northern Hemisphere peatlands shows regional and global trends during the past 6000 years. *The Holocene* **28**, 998–1010 (2018).
- Kaplina, T. N. History of permafrost strata of northern Yakutia in the Late Cenozoic. in *History of the Development of Permafrost Deposits of Eurasia* 153–181 (Nauka, 1981).
- Sher, A. *Pleistocene Mammals and Stratigraphy of the Far Northeast USSR and North America*.
- Mackay, J. R. Some observations on the growth and deformation of epigenetic, syngenetic and anti-syngenetic ice wedges. *Permafrost Periglacial Process.* **1**, 15–29 (1990).
- Konishchev, V. N. Evolution of cryolithozone in the pleistocene and holocene. *Permafrost Response Econ. Dev. Environ. Secur. Nat. Resour.* **76**, 139–149 (2001).
- Wennrich, V. et al. Impact processes, permafrost dynamics, and climate and environmental variability in the terrestrial Arctic as inferred from the unique 3.6 Myr record of Lake El'gygytyn, far East Russia—a review. *Quat. Sci. Rev.* **147**, 221–244 (2016).

40. Brigham-Grette, J. et al. Pliocene warmth, polar amplification, and stepped Pleistocene cooling recorded in NE Arctic Russia. *Science* **340**, 1421–1427 (2013).
41. Westgate, J. & Froese, D. G. Stop 15: Quartz Creek: Pliocene ice wedges/Quartz Creek tephra (63° 46' N, 139° 03' W). in *Fieldguide to Quaternary Research in Central and Western Yukon Territory*. vol. 2 69–71 (Yukon Heritage Branch Occasional Papers in Earth Science).
42. Matheus, P., Begét, J., Mason, O. & Gelvin-Reymler, C. Late Pliocene to late Pleistocene environments preserved at the Palisades site, central Yukon River, Alaska. *Quat. Res.* **60**, 33–43 (2003).
43. Péwé, T. L., Westgate, J. A., Preece, S. J., Brown, P. M. & Leavitt, S. W. Late Pliocene Dawson cut forest bed and new tephrochronological findings in the Gold Hill Loess, east-central Alaska. *Geol. Soc. Am. Bull.* **121**, 294–320 (2009).
44. Schirrmeyer, L. et al. Late Quaternary paleoenvironmental records from the western Lena Delta, arctic Siberia. *Palaeogeogr. Palaeoclimatol. Palaeoecol.* **299**, 175–196 (2011).
45. Strauss, J. et al. Deep Yedoma permafrost: a synthesis of depositional characteristics and carbon vulnerability. *Earth-Sci. Rev.* **172**, 75–86 (2017).
46. Vandenbergh, J. et al. The Last Permafrost Maximum (LPM) map of the Northern Hemisphere: permafrost extent and mean annual air temperatures, 25–17 ka BP. *Boreas* **43**, 652–666 (2014).
47. Saito, K. et al. LGM permafrost distribution: how well can the latest PMIP multi-model ensembles perform reconstruction? *Clim. Past* **9**, 1697–1714 (2013).
48. Saito, K. et al. Evaluation of LPM permafrost distribution in NE Asia reconstructed and downscaled from GCM simulations. *Boreas* **43**, 733–749 (2014).
49. Lindgren, A., Hugelius, G., Kuhry, P., Christensen, T. R. & Vandenbergh, J. GIS-based maps and area estimates of northern hemisphere permafrost extent during the last glacial maximum. *Permafrost. Periglac. Process.* **27**, 6–16 (2016).
50. Obu, J. et al. Northern Hemisphere permafrost map based on TTOP modelling for 2000–2016 at 1 km<sup>2</sup> scale. *Earth-Sci. Rev.* **193**, 299–316 (2019).
51. Lindgren, A., Hugelius, G. & Kuhry, P. Extensive loss of past permafrost carbon but a net accumulation into present-day soils. *Nature* **560**, 219–222 (2018).
52. Overduin, P. P. et al. Submarine permafrost map in the Arctic modeled using 1-D transient heat flux (supermap). *J. Geophys. Res. Oceans* **124**, 3490–3507 (2019).
53. Sayedi, S. S. et al. Subsea permafrost carbon stocks and climate change sensitivity estimated by expert assessment. *Environ. Res. Lett.* **15**, 124075 (2020).
54. Cronin, T. M. Rapid sea-level rise. *Quat. Sci. Rev.* **56**, 11–30 (2012).
55. Bauch, H. A. et al. Chronology of the Holocene transgression at the North Siberian margin. *Glob. Planet. Change* **31**, 125–139 (2001).
56. Cronin, T. M. et al. Deglacial sea level history of the East Siberian Sea and Chukchi Sea margins. *Clim. Past* **13**, 1097–1110 (2017).
57. Romanovskii, N. N. & Hubberten, H.-W. Results of permafrost modelling of the lowlands and shelf of the Laptev Sea region, Russia. *Permafrost. Periglac. Process.* **12**, 191–202 (2001).
58. Kuhry, P. Palsa and peat plateau development in the Hudson Bay Lowlands, Canada: timing, pathways and causes. *Boreas* **37**, 316–327 (2008).
59. Angelopoulos, M., Overduin, P. P., Miesner, F., Grigoriev, M. N. & Vasiliev, A. A. Recent advances in the study of Arctic submarine permafrost. *Permafrost. Periglac. Process.* **31**, 442–453 (2020).
60. Stevens, C. W., Moorman, B. J., Solomon, S. M. & Hugenholtz, C. H. Mapping subsurface conditions within the near-shore zone of an Arctic delta using ground penetrating radar. *Cold Reg. Sci. Technol.* **56**, 30–38 (2009).
61. Stevens, C. W., Moorman, B. J. & Solomon, S. M. Modeling ground thermal conditions and the limit of permafrost within the nearshore zone of the Mackenzie Delta, Canada. *J. Geophys. Res. Earth Surf.* **115**, F04027 (2010).
62. Brothers, L. L., Hart, P. E. & Ruppel, C. D. Minimum distribution of subsea ice-bearing permafrost on the US Beaufort Sea continental shelf. *Geophys. Res. Lett.* **39**, L15501 (2012).
63. Nicolsky, D. J. et al. Modeling sub-sea permafrost in the East Siberian Arctic Shelf: the Laptev Sea region. *J. Geophys. Res. Earth Surf.* **117**, F03028 (2012).
64. Angelopoulos, M. et al. Onshore thermokarst primes subsea permafrost degradation. *Geophys. Res. Lett.* **48**, e2021GL093881 (2021).
65. Overduin, P. P. et al. Coastal dynamics and submarine permafrost in shallow water of the central Laptev Sea, East Siberia. *Cryosphere* **10**, 1449–1462 (2016).
66. Velichko, A. A. et al. Climate changes in East Europe and Siberia at the Late glacial–holocene transition. *Quat. Int.* **91**, 75–99 (2002).
67. Vaks, A. et al. Speleothems reveal 500,000-year history of Siberian permafrost. *Science* **340**, 183–186 (2013).
68. Biller-Celander, N. et al. Increasing Pleistocene permafrost persistence and carbon cycle conundrums inferred from Canadian speleothems. *Sci. Adv.* **7**, eabe5799 (2021).
69. Schirrmeyer, L., Oezen, D. & Geyh, M. A. 230Th/U dating of frozen peat, Bol'shoy Lyakhovskiy Island (Northern Siberia). *Quat. Res.* **57**, 253–258 (2002).
70. Andreev, A. A. et al. Late Saalian and Eemian palaeoenvironmental history of the Bol'shoy Lyakhovskiy Island (Laptev Sea region, Arctic Siberia). *Boreas* **33**, 319–348 (2004).
71. Froese, D. G., Westgate, J. A., Reyes, A. V., Enkin, R. J. & Preece, S. J. Ancient permafrost and a future, warmer Arctic. *Science* **321**, 1648–1648 (2008).
72. Vaks, A. et al. Palaeoclimate evidence of vulnerable permafrost during times of low sea ice. *Nature* **577**, 221–225 (2020).
73. Wetterich, S. et al. Eemian and late glacial/Holocene palaeoenvironmental records from permafrost sequences at the Dmitry Laptev Strait (NE Siberia, Russia). *Palaeogeogr. Palaeoclimatol. Palaeoecol.* **279**, 73–95 (2009).
74. Ewing, S. A. et al. Long-term anoxia and release of ancient, labile carbon upon thaw of Pleistocene permafrost. *Geophys. Res. Lett.* **42**, 10–730 (2015).
75. Murton, J. B. et al. A multimethod dating study of ancient permafrost, Batagay megaslump, east Siberia. *Quat. Res.* **105**, 1–22 (2022).
76. Lunardini, V. J. Permafrost formation time. (1995).
77. van der Valk, T. et al. Million-year-old DNA sheds light on the genomic history of mammoths. *Nature* **591**, 265–269 (2021).
78. Snyder, C. W. Evolution of global temperature over the past two million years. *Nature* **538**, 226–228 (2016).
79. Raymo, M. E. & Mitrovica, J. X. Collapse of polar ice sheets during the stage 11 interglacial. *Nature* **483**, 453–456 (2012).
80. Dutton, A. et al. Sea-level rise due to polar ice-sheet mass loss during past warm periods. *Science* **349**, aaa4019 (2015).
81. Lacelle, D., Fontaine, M., Pellerin, A., Kokelj, S. V. & Clark, I. D. Legacy of holocene landscape changes on soil biogeochemistry: a perspective from paleo-active layers in Northwestern Canada. *J. Geophys. Res. Biogeosci.* **124**, 2662–2679 (2019).
82. Harry, D. G. & Gozdzik, J. S. Ice wedges: growth, thaw transformation, and palaeoenvironmental significance. *J. Quat. Sci.* **3**, 39–55 (1988).
83. Coulombe, S., Fortier, D., Lacelle, D., Kanevskiy, M. & Shur, Y. Origin, burial and preservation of late Pleistocene-age glacier ice in Arctic permafrost (Bylot Island, NU, Canada). *Cryosphere* **13**, 97–111 (2019).
84. Lacelle, D., Lauriol, B., Clark, I. D., Cardyn, R. & Zdanowicz, C. Nature and origin of a Pleistocene-age massive ground-ice body exposed in the Chapman Lake moraine complex, central Yukon Territory, Canada. *Quat. Res.* **68**, 249–260 (2007).
85. Ingólfsson, O. & Lokrantz, H. Massive ground ice body of glacial origin at Yugorski Peninsula, arctic Russia. *Permafrost. Periglac. Process.* **14**, 199–215 (2003).
86. Ehlers, J., Astakhov, V., Gibbard, P. L., Mangerud, J. & Svendsen, J. I. GLACIATIONS | middle pleistocene in Eurasia. *Encyclopedia of Quaternary Science* 172–179 (Elsevier, 2013). <https://doi.org/10.1016/B978-0-444-53643-3.00123-0>.
87. Jorgenson, M. T. et al. Resilience and vulnerability of permafrost to climate change. *Can. J. For. Res.* **40**, 1219–1236 (2010).
88. Zimov, S. A., Schuur, E. A. & Chapin, F. S. III Permafrost and the global carbon budget. *Science* **312**, 1612–1613 (2006).
89. Zimov, S. A. et al. Permafrost carbon: stock and decomposability of a globally significant carbon pool. *Geophys. Res. Lett.* **33**, L20502 (2006).
90. Zech, R., Huang, Y., Zech, M., Tarozo, R. & Zech, W. High carbon sequestration in Siberian permafrost loess-paleosols during glacials. *Clim. Past* **7**, 501–509 (2011).
91. Turetsky, M. R. et al. Carbon release through abrupt permafrost thaw. *Nat. Geosci.* **13**, 138–143 (2020).
92. Walter, K. M., Edwards, M. E., Grosse, G., Zimov, S. A. & Chapin, F. S. III Thermokarst lakes as a source of atmospheric CH<sub>4</sub> during the last deglaciation. *science* **318**, 633–636 (2007).
93. Brosius, L. S. et al. Spatiotemporal patterns of northern lake formation since the Last Glacial Maximum. *Quat. Sci. Rev.* **253**, 106773 (2021).
94. Jones, M. C. et al. Rapid carbon loss and slow recovery following permafrost thaw in boreal peatlands. *Glob. Change Biol.* **23**, 1109–1127 (2017).
95. Heffernan, L., Estop-Aragonés, C., Knorr, K.-H., Talbot, J. & Olefeldt, D. Long-term impacts of permafrost thaw on carbon storage in peatlands: Deep losses offset by surficial accumulation. *J. Geophys. Res. Biogeosci.* **125**, e2019JG005501 (2020).
96. Tesi, T. et al. Massive remobilization of permafrost carbon during post-glacial warming. *Nat. Commun.* **7**, 13653 (2016).
97. Winterfeld, M. et al. Deglacial mobilization of pre-aged terrestrial carbon from degrading permafrost. *Nat. Commun.* **9**, 3666 (2018).
98. Martens, J. et al. Remobilization of old permafrost carbon to Chukchi Sea sediments during the end of the last deglaciation. *Glob. Biogeochem. Cycles* **33**, 2–14 (2019).
99. Meyer, V. D. et al. Permafrost-carbon mobilization in Beringia caused by deglacial meltwater runoff, sea-level rise and warming. *Environ. Res. Lett.* **14**, 085003 (2019).
100. Martens, J. et al. Remobilization of dormant carbon from Siberian-Arctic permafrost during three past warming events. *Sci. Adv.* **6**, eabb6546 (2020).

101. Gaglioti, B. V. et al. Radiocarbon age-offsets in an arctic lake reveal the long-term response of permafrost carbon to climate change. *J. Geophys. Res. Biogeosci.* **119**, 1630–1651 (2014).
102. Wild, B. et al. Rivers across the Siberian Arctic unearth the patterns of carbon release from thawing permafrost. *Proc. Natl. Acad. Sci.* **116**, 10280–10285 (2019).
103. Wadhams, J. L., Tranter, M., Tulaczyk, S. & Sharp, M. Subglacial methanogenesis: a potential climatic amplifier? *Glob. Biogeochem. Cycles* **22**, GB2021 (2008).
104. Anthony, K. W. et al. A shift of thermokarst lakes from carbon sources to sinks during the Holocene epoch. *Nature* **511**, 452–456 (2014).
105. Jones, M. C., Grosse, G., Jones, B. M. & Walter Anthony, K. Peat accumulation in drained thermokarst lake basins in continuous, ice-rich permafrost, northern Seward Peninsula, Alaska. *J. Geophys. Res. Biogeosci.* **117**, G00M07 (2012).
106. Treat, C. C. et al. Widespread global peatland establishment and persistence over the last 130,000 y. *Proc. Natl. Acad. Sci.* **116**, 4822–4827 (2019).
107. Olefeldt, D. et al. Circumpolar distribution and carbon storage of thermokarst landscapes. *Nat. Commun.* **7**, 13043 (2016).
108. Osman, M. B. et al. Globally resolved surface temperatures since the Last Glacial Maximum. *Nature* **599**, 239–244 (2021).
109. Kleinen, T., Mikolajewicz, U. & Brovkin, V. Terrestrial methane emissions from the Last Glacial Maximum to the preindustrial period. *Clim. Past* **16**, 575–595 (2020).
110. Brosius, L. S. et al. Permafrost carbon contribution to the deglacial methane budget. *Commun. Earth Environ.* <https://doi.org/10.1038/s43247-023-00930-2>.
111. Crichton, K. A., Bouttes, N., Roche, D. M., Chappellaz, J. & Krinner, G. Permafrost carbon as a missing link to explain CO<sub>2</sub> changes during the last deglaciation. *Nat. Geosci.* **9**, 683–686 (2016).
112. Köhler, P., Knorr, G. & Bard, E. Permafrost thawing as a possible source of abrupt carbon release at the onset of the Bölling/Allerød. *Nat. Commun.* **5**, 5520 (2014).
113. Sowers, T. Atmospheric methane isotope records covering the Holocene period. *Quat. Sci. Rev.* **29**, 213–221 (2010).
114. Bock, M. et al. Glacial/interglacial wetland, biomass burning, and geologic methane emissions constrained by dual stable isotopic CH<sub>4</sub> ice core records. *Proc. Natl. Acad. Sci.* **114**, E5778–E5786 (2017).
115. Dean, J. F. et al. Abundant pre-industrial carbon detected in Canadian Arctic headwaters: implications for the permafrost carbon feedback. *Environ. Res. Lett.* **13**, 034024 (2018).
116. Elder, C. D. et al. Greenhouse gas emissions from diverse Arctic Alaskan lakes are dominated by young carbon. *Nat. Clim. Change* **8**, 166–171 (2018).
117. Schädel, C. et al. Potential carbon emissions dominated by carbon dioxide from thawed permafrost soils. *Nat. Clim. Change* **6**, 950–953 (2016).
118. Broecker, W. & Barker, S. A 190‰ drop in atmosphere's  $\delta^{14}\text{C}$  during the “Mystery Interval” (17.5 to 14.5 kyr). *Earth Planet. Sci. Lett.* **256**, 90–99 (2007).
119. Marcott, S. A. et al. Centennial-scale changes in the global carbon cycle during the last deglaciation. *Nature* **514**, 616–619 (2014).
120. Mann, D. H., Peteet, D. M., Reanier, R. E. & Kunz, M. L. Responses of an arctic landscape to Lateglacial and early Holocene climatic changes: the importance of moisture. *Quat. Sci. Rev.* **21**, 997–1021 (2002).
121. Mann, D. H., Groves, P., Reanier, R. E. & Kunz, M. L. Floodplains, permafrost, cottonwood trees, and peat: What happened the last time climate warmed suddenly in arctic Alaska? *Quat. Sci. Rev.* **29**, 3812–3830 (2010).
122. Fraser, R. H. et al. Climate sensitivity of high Arctic permafrost terrain demonstrated by widespread ice-wedge thermokarst on Banks Island. *Remote Sens.* **10**, 954 (2018).
123. Jones, M. K. W., Pollard, W. H. & Jones, B. M. Rapid initialization of retrogressive thaw slumps in the Canadian high Arctic and their response to climate and terrain factors. *Environ. Res. Lett.* **14**, 055006 (2019).
124. French, H. & Shur, Y. The principles of cryostratigraphy. *Earth-Sci. Rev.* **101**, 190–206 (2010).
125. Morgenstern, A., Grosse, G., Günther, F., Fedorova, I. & Schirmermeister, L. Spatial analyses of thermokarst lakes and basins in Yedoma landscapes of the Lena Delta. *Cryosphere* **5**, 849–867 (2011).
126. McGuire, A. D. et al. Dependence of the evolution of carbon dynamics in the northern permafrost region on the trajectory of climate change. *Proc. Natl. Acad. Sci.* **115**, 3882–3887 (2018).
127. Jones, M. C. & Yu, Z. Rapid deglacial and early Holocene expansion of peatlands in Alaska. *Proc. Natl. Acad. Sci.* **107**, 7347–7352 (2010).
128. Smith, L. C. et al. Siberian peatlands a net carbon sink and global methane source since the early Holocene. *Science* **303**, 353–356 (2004).
129. Byun, E., Sato, H., Cowling, S. A. & Finkelstein, S. A. Extensive wetland development in mid-latitude North America during the Bölling–Allerød. *Nat. Geosci.* **14**, 30–35 (2021).
130. Ulrich, M., Grosse, G., Strauss, J. & Schirmermeister, L. Quantifying wedge-ice volumes in Yedoma and thermokarst basin deposits. *Permafrost. Periglac. Process.* **25**, 151–161 (2014).
131. Kanevskiy, M. et al. Ground ice in the upper permafrost of the Beaufort Sea coast of Alaska. *Cold Reg. Sci. Technol.* **85**, 56–70 (2013).
132. O'Neill, H. B., Wolfe, S. A. & Duchesne, C. New ground ice maps for Canada using a paleogeographic modelling approach. *The Cryosphere* **13**, 753–773 (2019).
133. Overland, J. E. et al. Surface air temperature. *Arct. Rep. Card* **2015**, 10–16 (2015).
134. Williams, M. et al. Boreal permafrost thaw amplified by fire disturbance and precipitation increases. *Environ. Res. Lett.* **15**, 114050 (2020).
135. Douglas, T. A., Turetsky, M. R. & Koven, C. D. Increased rainfall stimulates permafrost thaw across a variety of Interior Alaskan boreal ecosystems. *Npj Clim. Atmos. Sci.* **3**, 28 (2020).
136. Shakhova, N. et al. Ebullition and storm-induced methane release from the East Siberian Arctic Shelf. *Nat. Geosci.* **7**, 64–70 (2014).
137. Steinbach, J. et al. Source apportionment of methane escaping the subsea permafrost system in the outer Eurasian Arctic Shelf. *Proc. Natl. Acad. Sci.* **118**, e2019672118 (2021).
138. Rachold, V. et al. Nearshore Arctic subsea permafrost in transition. *Eos Trans. Am. Geophys. Union* **88**, 149–150 (2007).
139. Shakhova, N. et al. Extensive methane venting to the atmosphere from sediments of the East Siberian Arctic Shelf. *Science* **327**, 1246–1250 (2010).
140. Andreassen, K. et al. Massive blow-out craters formed by hydrate-controlled methane expulsion from the Arctic seafloor. *Science* **356**, 948–953 (2017).
141. Chuvilin, E. et al. A Gas-emission crater in the Erkuta River valley, Yamal Peninsula: characteristics and potential formation model. *Geosciences* **10**, 170 (2020).
142. Walter Anthony, K. M., Anthony, P., Grosse, G. & Chanton, J. Geologic methane seeps along boundaries of Arctic permafrost thaw and melting glaciers. *Nat. Geosci.* **5**, 419–426 (2012).
143. Sullivan, T. D. et al. Influence of permafrost thaw on an extreme geologic methane seep. *Permafrost. Periglac. Process.* **32**, 484–502 (2021).
144. Tierney, J. E. et al. Glacial cooling and climate sensitivity revisited. *Nature* **584**, 569–573 (2020).
145. Jones, M. C., Berkelhammer, M., Keller, K. J., Yoshimura, K. & Wooller, M. J. High sensitivity of Bering Sea winter sea ice to winter insolation and carbon dioxide over the last 5500 years. *Sci. Adv.* **6**, eaaz9588 (2020).
146. Lawrence, D. M., Slater, A. G., Tomas, R. A., Holland, M. M. & Deser, C. Accelerated Arctic land warming and permafrost degradation during rapid sea ice loss. *Geophys. Res. Lett.* **35**, L11506 (2008).
147. Amante, C. & Eakins, B. W. *ETOPO1 Arc-Minute Global Relief Model: Procedures, Data Sources and Analysis* (NOAA Tech. Memo. NESDIS NGDC-24, Mar. Geol. Geophys. Div., National Geophys. Data Center, Natl. Ocean. Atmos. Admin. (NOAA), Boulder, CO, USA, 2009).
148. Dangendorf, S. et al. Persistent acceleration in global sea-level rise since the 1960s. *Nat. Clim. Change* **9**, 705–710 (2019).
149. Notz, D. & Stroeve, J. Observed Arctic sea-ice loss directly follows anthropogenic CO<sub>2</sub> emission. *Science* **354**, 747–750 (2016).
150. Jones, B. M. et al. A decade of remotely sensed observations highlight complex processes linked to coastal permafrost bluff erosion in the Arctic. *Environ. Res. Lett.* **13**, 115001 (2018).
151. Vonk, J. E. et al. Activation of old carbon by erosion of coastal and subsea permafrost in Arctic Siberia. *Nature* **489**, 137–140 (2012).
152. Tanski, G. et al. Rapid CO<sub>2</sub> release from eroding permafrost in seawater. *Geophys. Res. Lett.* **46**, 11244–11252 (2019).
153. Brown, J., Ferris Jr., O. J., Heginbottom, J. A. & Melnikov, E. S. Circum-Arctic map of permafrost and ground-ice conditions. Circum-Pacific Map 45. <https://pubs.er.usgs.gov/publication/cp45> (1997) <https://doi.org/10.3133/cp45>.
154. Ehlers, J., Gibbard, P. L. & Hughes, P. D. *Developments in Quaternary Sciences: Quaternary Glaciations-Extent and Chronology: A Closer Look*. Vol. **15**, 2–1108 (Elsevier, 2011).
155. Batchelor, C. L. et al. The configuration of Northern Hemisphere ice sheets through the Quaternary. *Nat. Commun.* **10**, 3713 (2019).
156. Loulergue, L. et al. Orbital and millennial-scale features of atmospheric CH<sub>4</sub> over the past 800,000 years. *Nature* **453**, 383–386 (2008).
157. Bereiter, B. et al. Revision of the EPICA Dome C CO<sub>2</sub> record from 800 to 600 kyr before present. *Geophys. Res. Lett.* **42**, 542–549 (2015).
158. Lisiecki, L. E. & Raymo, M. E. A Pliocene-Pleistocene stack of 57 globally distributed benthic  $\delta^{18}\text{O}$  records. *Paleoceanography* **20**, PA1003 (2005).
159. Reimer, P. J. et al. The IntCal20 Northern Hemisphere radiocarbon age calibration curve (0–55 cal kBP). *Radiocarbon* **62**, 725–757 (2020).
160. Köhler, P., Nehrbass-Ahles, C., Schmitt, J., Stocker, T. F. & Fischer, H. A 156 kyr smoothed history of the atmospheric greenhouse gases CO<sub>2</sub>, CH<sub>4</sub>, and N<sub>2</sub>O and their radiative forcing. *Earth Syst. Sci. Data* **9**, 363–387 (2017).
161. Schmitt, J. Rise from ice cores 2 carbon isotope constraints on the deglacial CO<sub>2</sub>. *Science* **1217161**, 336 (2012).

## Acknowledgements

The authors thank NSF for support through the P2C2 program (1903735). M.J. was supported by the USGS Climate R&D Program. C.T. was additionally supported by ERC FluxWin. G.G. was additionally supported by BMBF KoPf (03F0764B) and BMBF KoPf Synthesis (03F0834B). We thank Lutz Schirmermeister and Thomas Opel for discussing field evidence of ancient permafrost sites in Siberia. Tom Cronin and Laura Gemery

reviewed earlier versions of this manuscript. We thank Victor Brovkin and an anonymous reviewer for improving the final manuscript.

### Author contributions

M.C.J. conceived of the study and wrote the manuscript, G.G., M.R.T., K.W.A, C.T., and L.B. contributed writing, M.C.J. and G.G. compiled the data.

### Competing interests

The authors declare no competing interests.

### Additional information

**Supplementary information** The online version contains supplementary material available at <https://doi.org/10.1038/s43247-023-00886-3>.

**Correspondence** and requests for materials should be addressed to Miriam C. Jones.

**Peer review information** *Communications Earth & Environment* thanks Victor Brovkin and the other, anonymous, reviewer(s) for their contribution to the peer review of this work. Primary Handling Editor: Aliénor Lavergne.

**Reprints and permission information** is available at <http://www.nature.com/reprints>

**Publisher's note** Springer Nature remains neutral with regard to jurisdictional claims in published maps and institutional affiliations.



**Open Access** This article is licensed under a Creative Commons Attribution 4.0 International License, which permits use, sharing, adaptation, distribution and reproduction in any medium or format, as long as you give appropriate credit to the original author(s) and the source, provide a link to the Creative Commons licence, and indicate if changes were made. The images or other third party material in this article are included in the article's Creative Commons licence, unless indicated otherwise in a credit line to the material. If material is not included in the article's Creative Commons licence and your intended use is not permitted by statutory regulation or exceeds the permitted use, you will need to obtain permission directly from the copyright holder. To view a copy of this licence, visit <http://creativecommons.org/licenses/by/4.0/>.

This is a U.S. Government work and not under copyright protection in the US; foreign copyright protection may apply 2023